3-1-2011

A Faceted Magnetron Concept Using Field Emission Cathodes

Jim Browning
Boise State University

Jack Watrous
NumerEx

A Faceted Magnetron Concept Using Field Emission Cathodes

Jim Browning
Boise State University

Jack Watrous
NumerEx

A magnetron concept using field emission cathodes has been modeled with the Air Force Research Laboratory particle-in-cell code ICEPIC and the 2D particle trajectory simulation Lorentz2E. In this approach, field emitters are used to provide a distributed cathode in place of a traditional thermionic cathode. The emitters are placed below the interaction space in a shielded structure. The cathode is comprised of facet plates with slits to protect the emitters. Simulation of an L-band rising sun magnetron shows that the faceted magnetron will oscillate using both five and ten facet cathodes. The startup times are very similar to that of a cylindrical cathode magnetron. The electron trajectories of the shielded slit structure have been modeled, and the results indicate that electrons can be injected through the slits and into the interaction space using lateral edge emitters and a pusher electrode design.

Introduction

High power microwave devices are used in a number of applications including radar, communications, defeat of improvised explosives, and other forms of electronic warfare[1]. Crossed-field devices such as magnetrons[2] and Crossed-Field Amplifiers[1] (CFAs) have long been used for a variety of these applications. These devices can provide very high power (GW) with applications over a wide frequency range.[1] Improvements in these types of devices could be beneficial in terms of improved power density, efficiency, phase-locking, reduced startup times, and high frequency operation (>100 GHz).

A conventional magnetron, operating with applied voltages in the few to tens kV range and supplying RF power in the few to hundreds kW range, is typically comprised of a coaxial structure with an electron-supplying cathode at the center and a slow-wave structure on the outside. Electrons supplied by the cathode undergo azimuthal drift in the applied axial magnetic field and applied radial electric field. Their collective motion seeds, then interacts with and supports a resonant mode of the combined slow-wave structure and anode-cathode gap geometry. The operating frequency is determined by synchronism between electron flow and electric fields in the resonant mode. Conventional magnetrons typically use thermionic[1] cathodes, but research is currently exploring field emission cathodes as the electron source.[1,3]

Thermionic cathodes, while robust and widely used, do present some disadvantages. The magnetron is turned on and off by application of the cathode bias, so a high voltage pulse (20kV to 500 kV) is necessary for very high power magnetrons. Other than application of the bias voltage, the standard design offers no means of temporal control over electron injection. Ion back bombardment of the cathode can damage the cathode and can keep the cathode in a heated, thermionically emitting state. We propose the use of gated, vacuum field emitter arrays in place of thermionic cathodes. To protect the emitters from the harsh environment of the magnetron interaction space including ion back bombardment, the emitters are placed below the interaction space in a shielded structure. The field emission cathode offers a number of possible advantages. The emitter arrays inherently provide a distributed cathode. The electrons can be turned on and off using the relatively low (<500 V) gate voltage of the field emitters. Since the field emitters can be used in arrays, it is possible to control spatially the current injection. The spatial modulation may allow improved performance by injection of electrons only at the optimal location in the device where the greatest interaction occurs. At lower frequencies (~1 GHz), it may be possible to modulate the electrons at the operating frequency. The temporal modulation could be used to control the frequency of oscillation and might allow phase locking of multiple magnetrons. However, gated field emitters have a number of disadvantages. Gated emitters have not been successfully deployed in any microwave products although prototypes have been successful.[4] Explosive field emitters have also been tested[3] for use in high power configurations. Even with a distributed cathode, high current densities (~1 A/cm^2) are needed, and gated field emitters have had lifetime issues at such high current densities. In this paper we describe this device concept and present modeling results of the shielded cathode structure using the electron trajectory simulation Lorentz2E[5] and of the magnetron using the Air Force Research Laboratory particle-in-cell code, ICEPIC.[6]

Device Concept

The proposed cylindrical magnetron is based on using gated field emitters placed in a shielded structure housed within the cathode to prevent ion back bombardment to the emitters and to keep the emitters out of the harsh, high electric field environment of the magnetron. Since the emitters must be fabricated on flat surfaces, the cathode is comprised of facet plates with slits. This concept is shown in Fig. 1. The design here shows a simple cavity magnetron with 8 cavities and 5 facet plates. Each facet has slits for electron injection. The front of each facet is a conductor which forms the sole electrode. This sole electrode is biased negative and sets the interaction space electric field. The electrode is subject to both ion and electron bombardment and must be robust. The gated field emitters are placed below the slits. The shielded emitter slit configuration is shown in Fig. 2. Here, the emitter arrays are placed on either side of a slit but back from the exit opening of the slit to prevent back bombardment. The emitters are lateral devices[7] which emit along the surface of the substrate. The device configuration shows lateral tips with symmetric gates. These emitters can be stacked with multiple layers to provide multiple emission sites. Hence, the emission sites comprise an area defined by both the length of the slit (axial direction) and the vertical distance of the emitter stack in order to provide the maximum number of emission sites. The lateral emission of electrons along the surface allows the entire emitter (tip and gate) to be placed back from the slit exit opening. A pusher electrode is biased negative relative to the sole electrode in order to direct the electrons out through the slit openings and into the interaction space and space charge hub. Hundreds of slits could be fabricated on a single facet by using standard micro-fabrication techniques.

Magnetron Modeling

The modeling effort consists of two parts. The first part of the modeling looks at the effect of a faceted cathode on magnetron oscillation using the 3D electromagnetic particle-in-cell code, ICEPIC. The second part includes electron trajectory modeling to look at the ability to inject electrons into the interaction space through a slit by using a pusher electrode. The results of the ICEPIC calculations are used as a starting point for the trajectory modeling.

ICEPIC Results

The primary goal of the ICEPIC simulations was to determine what effect the faceted cathode would have on magnetron behavior. At the inception of the simulation effort, the option to explore designs in both two and three dimensions was considered crucial. Two dimensional calculations can be performed roughly an order of magnitude more rapidly than three dimensional calculations, permitting a great deal more ground to be covered. Three dimensional calculations then provide a more in-depth, more detailed look at selected designs. The fundamental difficulty with 2D calculations of standard conventional magnetrons is that the desired π-mode is separated from the (π-1)-mode by such a narrow margin in frequency that getting the π-mode to dominate is difficult. The standard mechanism of strapping helps, but strapping is inherently three-dimensional. What is needed for 2D work is a design that gives the π-mode sufficient frequency separation for it to be dominant. The "rising sun" magnetron configuration[8] was chosen because of its inherently 2D structure and large frequency separation it affords the π-mode.

A cross-sectional view of the geometry is shown in Fig. 3. This figure shows results of a 3D calculation, including the RF magnetic field and electron spokes. . The selected rising sun configuration uses two cavity sizes with cavity radii of 6 and 10 cm. The mouths of both cavities are 10° wide in azimuth. The cathode radius is 1 cm; the anode inner radius is 2.24 cm, and the axial length is 5 cm. The cathode is biased at -22.2kV, and there is a 900 G applied magnetic field. A side view is shown in Fig. 4. The ends of the slow-wave-structure are open. The cathode is terminated at the downstream end with an expanded-radius section that keeps electrons confined to the central region; the upstream end of the cathode is treated similarly. At the upstream end (left), the cathode and anode come close together to create a coaxial transmission line that is used to introduce the applied voltage. Given the scope of this effort, an extractor was neither designed nor included in the calculations. This precludes determination of operating efficiency since there is no output power to compare to the input power.

For the ICEPIC simulations, the cell size was 0.05 cm in the transverse dimensions (X, Z) and was 0.1 cm in the axial dimension (Y) resulting in roughly 4.5 million cells. The time step size was 1.075×10^{-12} s. Fig. 3 shows both the development of a 5-spoke electron structure. The plot also shows a grey-scale contour plot of the oscillating part of the normal-to-the-plane magnetic field component. The field clearly changes phase by 180° from one cavity to the next. This, along with the electron flow structure, indicates π-mode operation. The operating frequency for this device is 1086 MHz.
The reference simulation shown in Fig. 3 was run using a simple cylindrical cathode with current emission distributed along the entire cathode surface. Electrons are introduced into the system through a space-charge-limited emission algorithm. The

space-charge-limited algorithm used in ICEPIC has been extensively validated against both theoretical predictions and experimental measurements.[9,10] The space charge limited current drawn during oscillation was calculated to be 16.3 A. The power draw was 362 kW. Shown in Fig. 5 are two different time periods during the simulation of the magnetron. In Fig. 5 (a) the electron hub is displayed at a time of 64.5 ns which is before oscillation occurs. In Fig. 5 (b) the spokes have clearly formed showing oscillation at a time of 183.8 ns. The frequency spectra from this magnetron as well as the two other cases are shown in Fig. 6. The spectra come from the gap voltage response in the magnetron, and based on the number of points used in the Fast Fourier Transform to obtain the spectra, the resolution in +/- 3.55 MHz. The 1086.0 MHz peak is very clear without any close competing modes visible.

A five-sided cathode was then dropped in as a replacement for the cylindrical cathode with all other parameters in the calculation unchanged. The corners of the facets are at a radius of 1 cm and each facet is 1.18 cm wide. The spoke formation results are shown in Fig. 7. Fig 7(a) shows four lobes dominating the pre-oscillation state (t = 52.7 ns). The four-lobed structure appears to be related to the combination of the cathode geometry and the cycloidal electron trajectories and will be the subject of future work. However, as shown in Fig. 7(b), after 127.9 ns, the magnetron has started oscillating, and there are five spokes as expected. The frequency of oscillation is still 1086.0 MHz, and the current draw and power are essentially the same. The simulations were repeated for a ten facet cathode with substantially similar results in terms of frequency and power of the magnetron. The frequency spectra for these two cases are also shown in Fig. 6; the results are clearly similar with the same oscillation frequency. These ICEPIC results were compared with a cold cavity, 2D calculation of the slow wave structure using SUPERFISH[11] for the three cathode geometries. SUPERFISH is a 2D, frequency domain, Eigen mode solver. While the SUPERFISH calculations for a cold, 2D case show a different resonant frequency then the 3D ICEPIC results (956.5 MHz vs. 1086.0 MHz), the SUPERFISH calculations also show a small frequency difference (< 4.1 MHz) among the three geometries. Hence, the faceted cathode structure does not significantly alter the oscillation frequency from the cylindrical cathode case, but there is a difference.

Another consideration is the magnetron start time. Fig. 8 shows the voltage envelope from the same gap from the three different calculations. The envelope is the curve obtained by connecting the local maxima of the raw voltage absolute value vs. time data. Fig. 9 shows the time history of the amplitude of the π-mode. In analyzing magnetron behavior, the response of any given gap voltage is typically not as interesting as the dynamic response of the ensemble of gap voltages relative to one another, as this is what determines mode structure. Mode amplitudes can be related to gap voltages through a simple Fourier analysis. Specifically, we take the gap voltages at each time and calculate the mode amplitudes

$$A_n(t) = \sum_{j=1}^{N} V_j\,(t)\cos\,(j\frac{2\pi n}{N})$$

where A_n is the amplitude of mode n, V_j is the gap voltage for cavity j, and N is the number of cavities. When a 10-cavity slow wave structure supports an rf field that changes phase by 180° from one cavity to the adjacent cavity(the π-mode), then the $n=5$ mode given by

$$A_5(t) = \sum_{j=1}^{N} V_j\,(t)(-1)^j$$

is the dominate mode. These results show that the five sided cathode starts oscillating sooner than the cylindrical cathode, but the ten sided cathode starts later. The difference in start time is less than 50 ns for the three cases. The π–mode amplitude mirrors the voltage envelope, indicating that the π–mode was dominant throughout the entire course of oscillatory behavior. These results are discussed in more detail later.

Shielded Slit Electron Trajectory Results

Lorentz2E is a 2D particle trajectory simulation which can include both space charge and surface charge effects. The simulation solves for the electric fields and uses a Runge-Kutta technique for the electron trajectory tracking. The simulation can be set to inject a fixed current with a user-determined number of electron rays containing a proportional fraction of that current. The primary objective of the electron trajectory modeling was to determine whether the shielded slit structure with pusher electrode could be used to inject electrons into the interaction space of the magnetron with little or no bombardment on insulating surfaces. Additional concerns include ion back bombardment within the slits, practical size and voltage limits on the structure, and initial energy of the electrons relative to the sole electrode. If in order for the electrons to be able to overcome the space charge hub, they must be born too negative with respect to the sole electrode, then most electrons will back bombard and collect on the sole or will enter back into other slits.

In the modeling effort a number of slit designs including large (~ 300 μm), medium (~40 μm), and small (~10 μm) were studied. In all of these configurations the simulation showed that it is possible to extract electrons through the slits. Some basic experiments, details of which will be presented in later papers, performed on large slits with lateral emitters also confirmed the simulation results. For this concept to be practical, the maximum current possible must be extracted from the field emission arrays, so the most effective approach is to use the smallest slits possible to allow for the greatest number of emitters. Therefore, the modeling described here is for an 8 μm slit exit opening.

The Lorentz2E magnetron model used in the simulations is shown in Fig. 10 and 11. Figure 10 shows the five sided faceted cathode with a smooth anode (the outer circle). The cathode has a 1 cm radius at the facet corner while the anode has a 2.24 cm radius. Each facet is 1.18 cm wide. There is a second inner circle in the figure representing a region of volume space charge. A volume space charge was set up in the simulation to represent an electron hub. The electron density was found from the ICEPIC calculations to have a peak value of $6x10^{10}$ cm^{-3}. The hub extends from a radius of 1 cm to 1.5 cm. Using an average radial difference of 0.3 cm and a cathode length of 5 cm, the total charge in the volume was estimated to be $-1.35x10^{-8}$ C. To be conservative, a total volume charge of -1.5 $x10^{-8}$ C was then used in the simulation to represent the charge hub. The ring of charge area can be seen in Fig. 10 as defined by the region between the five sided cathode and the inner circle. The Lorentz simulation can be run to include the space charge effects of the individual rays on adjacent rays; however the simulation will not allow both the ray charge and the simulated space charge hub at the same time. Therefore, the results shown here do not include ray space charge simultaneously with the hub charge. However, simulations with the ray space charge and no hub charge have been run and do not show significant effects on the ray trajectories at the slit exits at the current densities simulated. The sole electrode is set to -22.2 kV, and there is an axial magnetic field of 900 G. On the top facet a slit structure is placed near the left facet edge as indicated.

The expanded view of the slit structure is shown in Fig. 11 (a). Comprising the shielded slit structure are the emitters on each side of the slit as well as the gates, the pusher electrode, the dielectric wall, and the sole electrode. Because the simulation is 2D, the actual lateral emitter structure cannot be properly modeled. For simplicity, the stacked emitters were modeled as a line with a fixed injection current. The gate was modeled as block which allows electron transit. All other electrodes were defined as collectors. The slit exit is 8 μm across; the sole electrode is 2 μm thick. Thick electrodes are needed in order to handle the thermal loading and the ion back bombardment. The exposed dielectric is minimized to prevent charging. Also shown in the figure are the voltages for the electrodes and the emitters with the sole electrode biased at -22.2 kV, the emitters biased at -22.3 kV, the pusher at -22.3 kV, and the gate at -21.7 kV. These values are obtained from the simulation for the best extraction of the electrons out of the slit.

Fifty rays were used in the simulation with twenty five rays per side. Using a 20 μm pitch for the slits and a facet width of 1.18 cm, there would be over 500 slits per facet. For a five facet cathode and using the 16.3 A total emission current, the resulting current required per slit is 6.5 mA. Therefore, the 6.5 mA was split among fifty rays with a current of 0.13 mA/ray. The ray trajectories are shown in Fig. 11 (b). Here the rays can be seen leaving the emitter segment and transiting through the gate. As the rays move into the slit region, the field from the pusher electrode directs the electrons up through the slit. Note that the asymmetry in the ray trajectories (left to right side) is due to the magnetic field. In order to extract the electrons through the space charge hub, the modeling shows that the pusher electrode must be placed below (geometrically) the level of the field emitter; otherwise it was not possible to achieve extraction. Instead when the pusher electrode was biased more negative than the sole electrode, many of the electrons would turn back within the slit because the field near the emitter gate was too negative. In addition, the emitter electrons had to be born slightly more negative (100 eV) than the sole electrode to get extraction. The simulation shows that electrons can be pushed out of the slit and can overcome the hub space charge.

Fig. 10 shows rays emanating from a single slit. A maximum time was set in the simulation to stop the rays after three orbits. The electron trajectory undergoes a change in character every time it passes through the inner turning point; this variation is due to the mismatch between the period of the cycloidal orbit and the azimuthal variation in cathode geometry and tends to cause electrons to experience larger radial excursions than are seen with the cylindrical cathode. It is also clear that some rays collect on the sole electrode after an orbit. This collection is due to the electrons being generated at a more negative potential than the sole electrode and is undesirable. We have not shown multiple sets of rays from additional slits because of the difficulty in visually following the rays and because the results are substantially similar.

Results and Discussion

The ICEPIC calculations show no harmful effects in magnetron behavior due to changing the cathode shape from circular to either pentagonal or decagonal. However, several issues should be addressed.

First, the electron injection in the ICEPIC calculations assumes a simple distributed cathode with space charge limited emission. This model does not include either the electron energy and initial velocity distributions or the discrete nature of the emission sites associated with the shielded slit structure. Given slits with a 20 μm pitch and 8 μm exit width, 40% of the surface area of the sole electrode will emit. In addition, the electrons are born with varying angles of emission and will enter the interaction region with a relatively narrow distribution in velocity. These properties could affect magnetron performance. In future work we plan to generate the appropriate spatial and velocity distributions for ICEPIC input by using the results of the electron trajectory modeling in combination with actual experimental measurements.

Another issue is the four spatial nodes seen in the ICEPIC simulations prior to oscillation. These results are not yet understood and will be the subject of future work.

Third, ICEPIC results indicate that the cathode geometry has an effect on the start-up time. Prior work[12,13] has shown that the use of multiple cathodes (e.g., 3 smaller cathodes for a 6 cavity magnetron) can reduce start up time in relativistic magnetrons. The faceted cathode would be inherently such a structure and should in general be an improvement. Future efforts will explore the number of facets optimal for magnetron performance. Other considerations might be controlling the current spatially (axially and azimuthally) by using the addressable nature of the field emission arrays in order to improve performance. End losses for example could be limited with the axial spatial control to provide optimal performance, i.e. injecting electrons where they do the most good. Finally, the ability to inject electrons using gated field emitters could provide a tool for the study of the device physics. Temporal or spatial modulation could be used to generate device perturbations; the results of these perturbations could be measured with different diagnostics and compared with simulations in order to improve our understanding of the device.

The shield structures and their fabrication are a critical aspect of the device. The facets could be micro-fabricated in one integrated structure using thin film materials for the electrodes, dielectrics, and field emitters. Refractory materials such as tungsten are a good choice for electrode fabrication with either silicon dioxide or silicon nitride, depending upon details of the fabrication process, being good choices for the dielectric. The slit dielectric wall should be fabricated from or coated with a high resistivity material such as silicon. This surface would act as a charge-bleed layer to prevent surface-charge accumulation from ion and electron bombardment which could otherwise affect the injection of high current density beams into the interaction space. The process substrate must have sufficient thermal conductivity to allow for removal of the waste heat generated by the back bombarding species. Sputtered films should be avoided to prevent argon out-gassing. The facet edges will be a significant mechanical issue. The facets must be assembled onto a frame with smooth surfaces at the joints to prevent spurious emission sites.

For the 5 cm long device, the slit exit current density is approximately 1.64 A/cm^2. The emitters are on 2 sides of the slits, and there are multiple emission sites. Assuming one lateral emitter every 20 μm, there would be 2500 emitters per side. This calculation does not take into account stacked emitter sites. Using the required 6.5 mA current per slit, the average current per emitter would be 1.3 μA. Such values are reasonable for gated field emitters; arrays of lateral emitters have achieved average currents of over 3 μA per lateral tip[7] with a 10 μm tip pitch. If the stacked emitters can be used to increase the number of sites by a factor of 2 or 3, the current per emitter becomes quite achievable. Field emitters have not yet demonstrated long lifetimes at high current densities, although some success has been seen in microwave applications[4]; nevertheless lifetime issues are a critical limiting factor in this application and will be the subject of future work. In future work we plan to test lateral emitters in a shielded slit structure to determine whether high current density beams can be extracted in a dummy magnetron setup.

Summary and Conclusions

We have proposed a magnetron configuration in which gated field emitters are used as the cathode by placing the emitters in a shielded structure. To fabricate such a structure, a faceted cathode is required. Simulations using ICEPIC have shown that an L-band, 362 kW, faceted cathode magnetron will oscillate and perform essentially the same as a cylindrical cathode magnetron. Simulations of the shielded field emitter structure using a particle trajectory code have also shown that it is possible to extract electrons from the slit of the structure by using a pusher electrode placed physically below the field emitters and biased at least 100 V more negative that the sole electrode. The resulting electron rays have highly cycloidal orbits. Future work will include the use of measured and simulated electron energy and spatial distributions in ICEPIC as well as the experimental analysis of cathode facet test structures.

Acknowledgments

This research is supported by the Air Force Office of Scientific Research (AFOSR) under contract #FA9550-09-C-0141. The authors also acknowledge the support provided by T. Rowe and S. Shawver from Boise State University and the useful discussions with N. Kumar and M. Eaton of Stellar Micro Devices of Austin, TX.

References

[1]R.J. Barker, J.H. Booske, N.C. Luhmann, G.S. Nusionovich, *Modern Microwave and Millimeter-Wave Power Electronics* (IEEE Press, Piscataway, 2005).
[2] G.B. Collins, *Microwave Magnetron* (McGraw Hill, New York, 1948).
[3] D. A. Shiffler, J. Luginsland, M. Ruebush, M. LaCour, K. Golby, K. Cartwright, M. Haworth, and T. Spencer, IEEE Trans. on Plasma Sci. **32**, 1261 (2004).
[4] D.R. Whaley, R. Duggal, C.M. Armstrong, C.L. Bellew, C.E. Holland, C.A. Spindt, IEEE Trans. On Electr. Dev. **56**, 896 (2009).
[5]Integrated Engineering Software Inc. OERSTED, Users and Technical Manual, Version 1.0, 46-1313 Border Place, Winnipeg, Manitoba, Canada, R3H 0X4, 1992. Available: http://www.integratedsoft.com
[6]Peterkin and Luginsland, Comp. Sci. Engin. **4**, 42 (2002).
[7] K. Subramanian, W.P. Kang, J.L. Davidson, M.Howell, Diam. and Rel. Mat. **17**,786 (2008).
[8]R. R. Moats, "Investigation of Anode Structure in a Rising-Sun Magnetron," Technical Report No. 99; Research Laboratory of Electronics; Massachusetts Institute of Technology, May 18 (1949).
[9]J. J. Watrous, J. W. Luginsland, and G. E. Sasser III, Phys. Plasmas **8**, 289 (2001).
[10]J. J. Watrous, J. W. Luginsland, and M. H. Frese, Phys. Plasmas **8**, 4202 (2001).
[11]K. Halbach and R. F. Holsinger, Particle Accelerators **7,** 213 (1976).
[12]M.C. Jones, V.B. Neculaes, Y.Y. Lau, R.M. Gilgenbach, and W.M. White, Appl. Phys. Lett. **85,** 6332 (2004).
[13]M.C. Jones, V.B. Neculaes, Y.Y. Lau, R.M. Gilgenbach, W.M. White, B.W. Hoff, and N.M. Jordan, Appl. Phys. Lett. **87,** 081501 (2005).

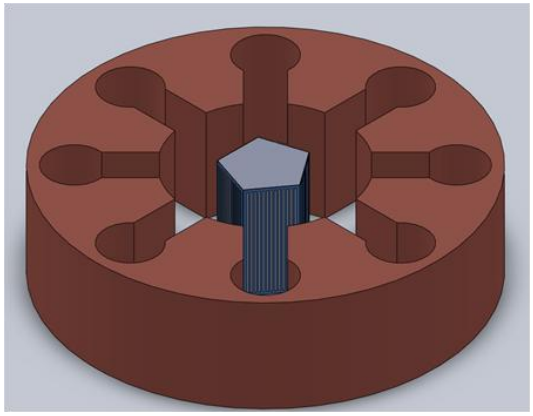

Figure 1. Faceted cathode magnetron concept for an 8 cavity magnetron

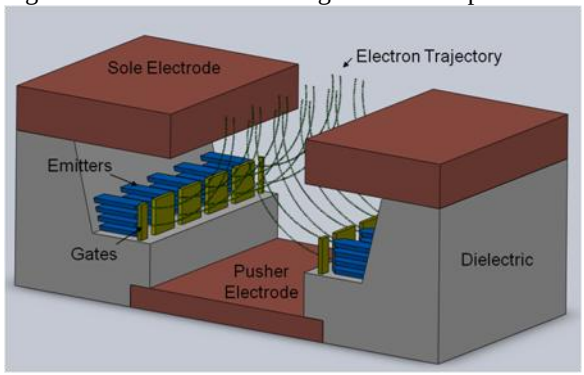

Figure 2. Shielded cathode slit showing stacked, lateral field emission tips on each side of the slit, a pusher electrode, the sole electrode, and electron trajectories

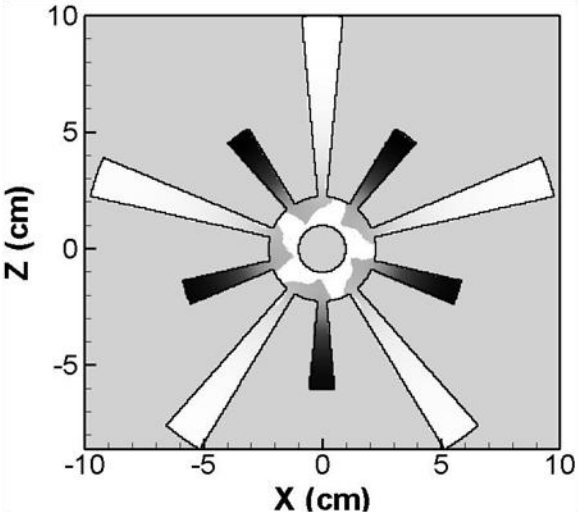

Figure 3. The rising sun magnetron model from the ICEPIC simulation showing 10 cavities of two different sizes. The cathode radius =1.0 cm, the anode inner radius=2.242 cm, the small cavity outer radius=6.0 cm, and the large cavity outer radius =10.0 cm.

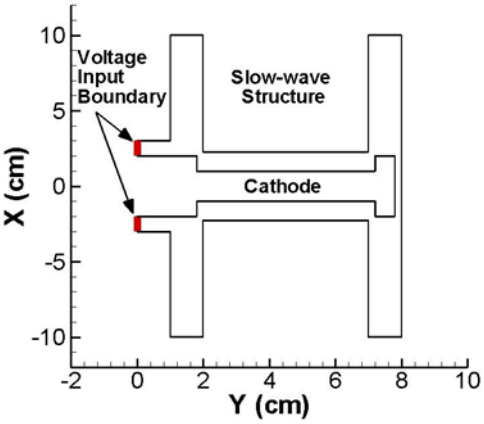

Figure 4. A side view of the rising sun magnetron used in the ICEPIC simulation.

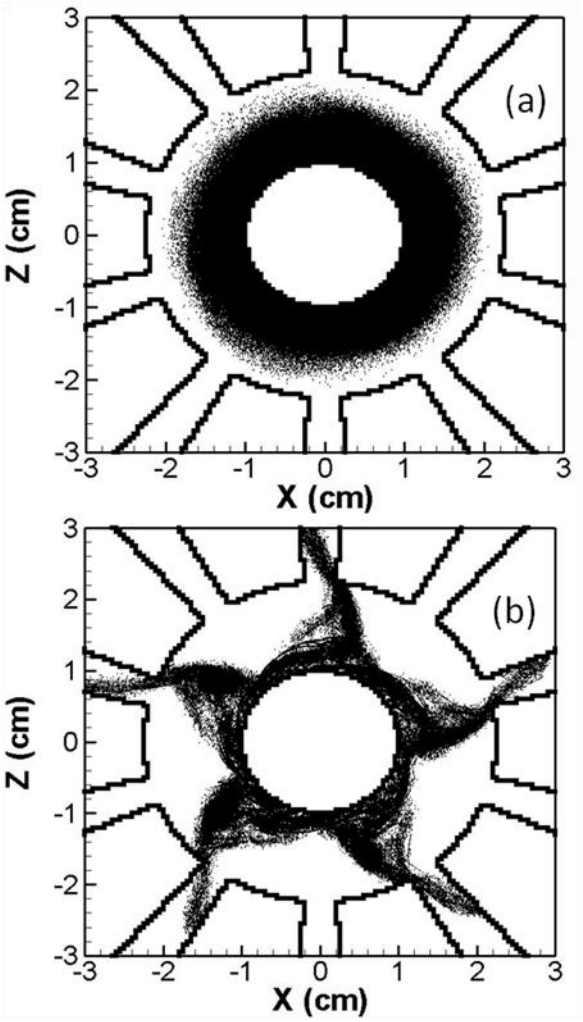

Figure 5. ICEPIC results for the cylindrical cathode at (a) 64.5 ns, before oscillation, and (b) 183.3 ns, after oscillation starts.

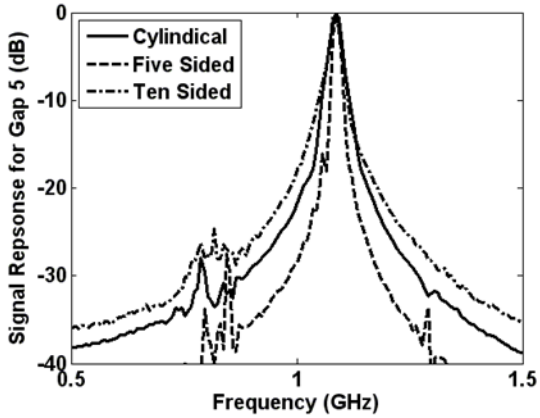

Figure 6. ICEPIC generated frequency spectra showing the clear 1086.0 MHz field at oscillation for the cylindrical, five sided, and ten sided cathodes.

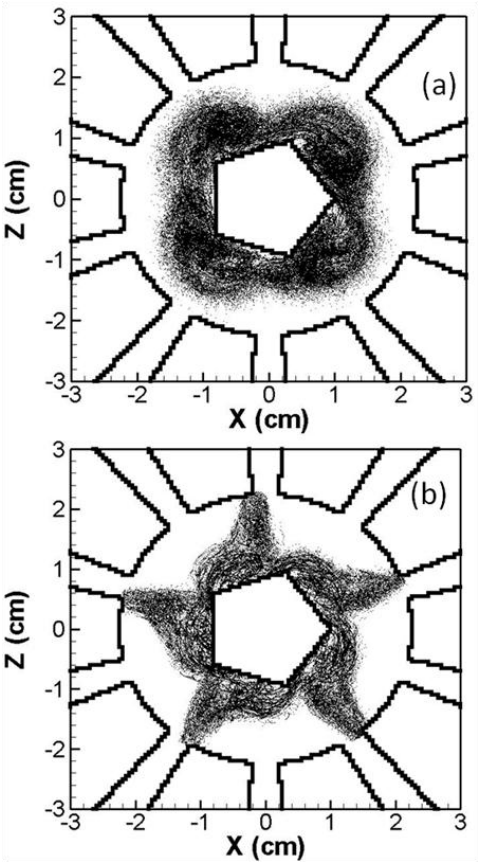

Figure 7. ICEPIC results for the five sided cathode at (a) 53.7 ns, before oscillation, with four nodes visible and at (b) 127.8 ns, after oscillation starts.

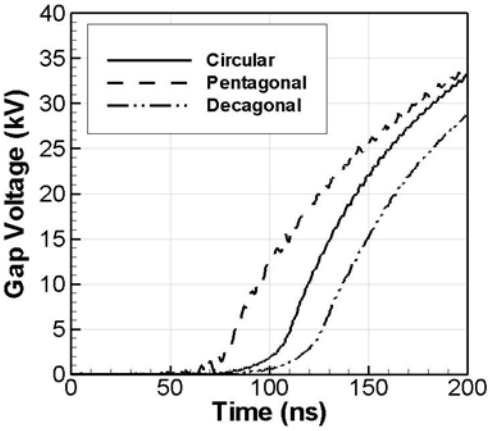

Figure 8. Amplitude of the 1086.0 MHz voltage output versus simulation time for the cylindrical, five sided, and ten sided cathodes.

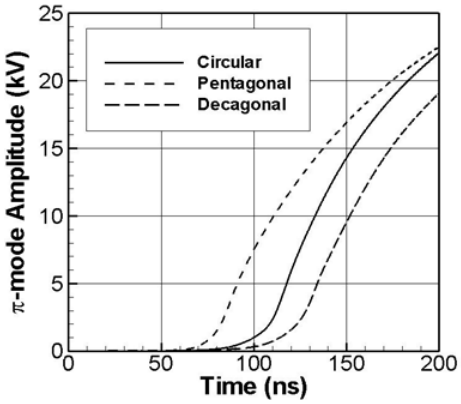

Figure 9. Time-history of the π-mode for the rising sun magnetron with cylindrical, five-sided, and ten-sided cathodes.

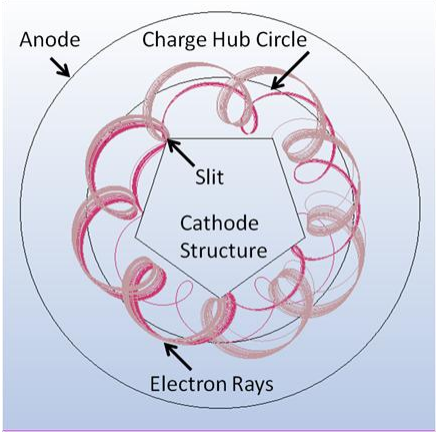

Figure 10. Magnetron model used in Lorentz2E for a five sided cathode with a smooth dummy anode showing electron ray traces from a shielded slit structure on the left hand side of the top facet. The outer circle is the anode and the inner circle defines a region of a volume electron charge representing the space charge hub.

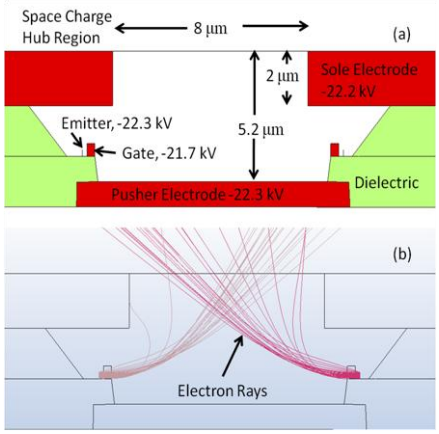

Figure 11. Lorentz model of the shielded cathode slit structure showing (a) the emitters on each side, a field emission gate transparent to electrons, a pusher electrode, the sole electrode, electrode voltages, and dimensions and (b) electron ray trajectories from the simulation.